

High-Temperature Quantum Oscillations of a Non-equilibrium Non-Fermi Liquid

Oles Matsyshyn,¹ Li-kun Shi,² and Inti Sodemann Villadiego³

¹*Division of Physics and Applied Physics, School of Physical and Mathematical Sciences, Nanyang Technological University, Singapore 637371*

²*Center for Quantum Matter, School of Physics, Zhejiang University, Hangzhou 310058, China*

³*Institut für Theoretische Physik, Universität Leipzig, Brüderstraße 16, 04103, Leipzig, Germany*
(Dated: December 29, 2025)

A periodically driven Fermi gas coupled to a simple boson bath reaches a non-equilibrium steady-state occupation with sharp non-analyticities at certain momenta. Here, we demonstrate that these non-analyticities behave as emergent Fermi surfaces by showing that they give rise to quantum oscillations of observables with a period controlled by the effective Fermi surface area enclosed by these non-analyticities. However, these oscillations have several striking differences with standard equilibrium quantum oscillations. For example, they remain non-analytic at finite temperatures, their amplitude can survive up to extremely high temperatures comparable to the frequency of the drive, and they can display non-monotonic temperature dependence completely at odds with standard Lifshits-Kosevich behavior.

Introduction. The Fermi surface is typically viewed as a characteristic of equilibrium Fermi liquids which is sharp only at zero temperature. However, recent studies have demonstrated that the steady state occupations of periodically driven Fermions can display non-analyticities that behave as emergent Fermi surfaces [1–3]. In particular, fermions driven periodically with a frequency Ω (i.e. by monochromatic light) and coupled to a local bosonic ohmic bath, display a jump of the second derivative at wave-vector $k_F^2/2m = \hbar\Omega$ [3] (see Fig.1), which remains sharp even when the bath is at finite temperature and gives rise to phenomena reminiscent to those of equilibrium non-Fermi liquids [3].

In this study, we will demonstrate that these non-analyticities behave as emergent Fermi surfaces by showing that they give rise to quantum oscillations in response to magnetic fields with a period controlled by their enclosed area in momentum space. However, we will show that many of the properties differ sharply from those of equilibrium Fermi liquids, further substantiating the idea that they behave like the Fermi surface of a non-equilibrium non-Fermi liquid state. For example, we will demonstrate that, amazingly, the quantum oscillations of these non-equilibrium states are non-analytic as a function of magnetic field even at finite temperature, and that their amplitude is a non-monotonic function of temperature that can survive up to extremely high temperatures comparable to the driving frequency, which is completely at odds with equilibrium behavior [4].

Periodically driven fermions coupled to a boson bath.

We consider a system of fermions driven by a time-periodic Hamiltonian $\hat{H}_e(t) = \hat{H}_e(t + T)$. This system is coupled via \hat{H}_{e-b} to a bosonic bath governed by \hat{H}_b , yielding the total Hamiltonian:

$$\hat{H}(t) = \hat{H}_e(t) + \hat{H}_b + \hat{H}_{e-b}, \quad (1)$$

where $\hat{H}_e(t) = \sum_{\alpha\beta} \langle \alpha | \hat{h}_t | \beta \rangle \hat{c}_\alpha^\dagger \hat{c}_\beta$, $\hat{H}_b = \sum_q \hbar\omega_q \hat{b}_q^\dagger \hat{b}_q$, and $\hat{H}_{e-b} = \sum_{q,\nu\eta} \langle \nu | \hat{\chi}_q | \eta \rangle \hat{b}_q \hat{c}_\nu^\dagger \hat{c}_\eta + \text{h.c.}$. Here, \hat{h}_t is the single-particle system Hamiltonian, and $\hat{\chi}_q$ describes

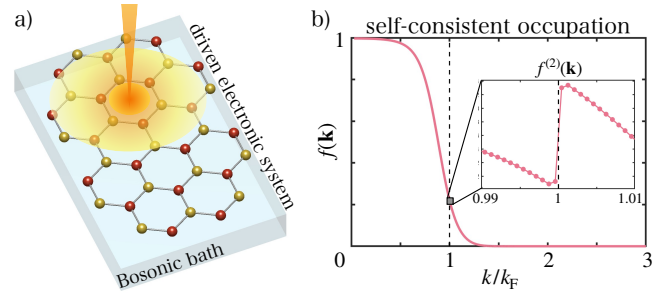


FIG. 1. (a) Electrons driven by light of frequency Ω and coupled to an ohmic boson bath, have an occupation of states (b) with a discontinuous second derivative at momentum $k_F^2/2m = \hbar\Omega$. Here we chosen $\bar{n}_e = n_e h/(m\Omega) = 0.8$, $\kappa^2 = e^2 |\mathcal{E}|^2/(m\hbar\Omega^3) = 0.04$.

the coupling to bath mode q . The operators \hat{c}_α^\dagger , \hat{c}_α (\hat{b}_q^\dagger , \hat{b}_q) create and annihilate fermions (bosons) in state $|\alpha\rangle$ (mode q). The bath is assumed to be in thermal equilibrium, with Bose-Einstein occupation $N_q = 1/(e^{\beta\hbar\omega_q} - 1)$ and temperature $k_B T_{\text{bath}} = 1/\beta$. The electron system, however, can be driven far from equilibrium through the periodic drive in $\hat{H}_e(t)$. Starting from the full quantum kinetic equation discussed in Refs.[3, 5], for the system one-body density matrix, $\rho_{\nu\eta} = \langle c_\eta^\dagger c_\nu \rangle$, which contains memory effects, one can prove that in the limit of weak system-bath coupling ($\chi_q \rightarrow 0$), the steady state of this matrix has Periodic Gibbs ensemble form [6–9]:

$$\hat{\rho}_t = \sum_\alpha f_\alpha |\psi_\alpha^F(t)\rangle \langle \psi_\alpha^F(t)|, \quad (2)$$

where $|\psi_\alpha^F(t)\rangle = e^{-i\epsilon_\alpha^F t} \sum_{n=-\infty}^{\infty} e^{-in\Omega t} |\phi_\alpha^n\rangle$ are the solutions of the time-dependent single particle Schrödinger equation for h_t , ϵ_α^F are the Floquet energies, and $\Omega = 2\pi/T$. This solution reflects the synchronization of the system with the external periodic drive. The occupations of the Floquet states f_α , which are time-independent and are obtained by solving the following Floquet-Boltzmann

equation:

$$\sum_{\beta} f_{\beta} \bar{f}_{\alpha} \langle W_t^{\alpha \rightarrow \beta} \rangle_T - \sum_{\beta} \bar{f}_{\beta} f_{\alpha} \langle W_t^{\beta \rightarrow \alpha} \rangle_T = 0, \quad (3)$$

where $\langle W_t^{\alpha \rightarrow \beta} \rangle \equiv \int_0^T (W_{e,t}^{\alpha \rightarrow \beta} + W_{a,t}^{\alpha \rightarrow \beta}) dt / T$ is the time averaged transition rate from state α to β and $\bar{f}_{\alpha} = 1 - f_{\alpha}$. The emission rate is given by:

$$\langle W_{e,t}^{\alpha \rightarrow \beta} \rangle = \frac{2\pi}{\hbar} \sum_{n,q} |V_{\alpha \rightarrow \beta}^n(q)|^2 \delta(\epsilon_{\beta}^F - \epsilon_{\alpha}^F + \hbar\omega_q + n\hbar\Omega), \quad (4)$$

$$|V_{\alpha \rightarrow \beta}^n(q)|^2 = (N_q + 1) \left| \sum_m \langle \phi_{\alpha}^m | \hat{\chi}_q | \phi_{\beta}^{m+n} \rangle \right|^2.$$

while the absorption rate $\langle W_{a,t}^{\alpha \rightarrow \beta} \rangle_T$ is obtained from Eq.(4) by substitution $N_q + 1 \rightarrow N_q$, $\omega_q \rightarrow -\omega_q$, $\hat{\chi} \rightarrow \hat{\chi}^{\dagger}$ [5]. The above results generalize the results of Ref.[3] to arbitrary periodically driven free fermion Hamiltonians with an arbitrary vertex coupling to a boson bath. Similar Floquet Boltzmann equations have also been derived in Refs.[10–13]. Notice that the above scattering rates obey a generalized form of Fermi’s Golden rule. This rule allows violations of Floquet energy conservation modulo Ω (Floquet umklapp). Crucially, these rates do not obey detailed balance. In the limit of vanishing amplitude of the drive, the Floquet wavefunction becomes static and $|\phi_{\alpha,n} \rangle \rightarrow \delta_{n0} |\phi_{\alpha,0} \rangle$, the *Floquet Fermi’s Golden Rule* reduces to the standard Fermi’s Golden Rule.

Floquet non-Fermi liquid at zero magnetic field. As demonstrated in Ref.[3], the steady-state of Fermions driven by monochromatic light and coupled to boson baths displays emergent non-analyticities at certain momenta which resemble the Fermi surfaces of a non-Fermi liquid. Let us review the nature of these states before generalizing to finite magnetic fields. We take a system of parabolic fermions subjected to uniform monochromatic radiation:

$$\hat{h}_t = \left[\mathbf{p} - \frac{e}{\hbar} \mathbf{A}(t) \right]^2 / (2m), \quad (5)$$

where $\mathbf{A}(t) = -i\Omega^{-1} \mathcal{E}_+ \exp(-i\Omega t) + c.c.$ with $\mathcal{E}_- = (\mathcal{E}_+)^*$. The intensity of the light will be parametrized by the dimensionless constant $\kappa^2 = e^2 |\mathcal{E}|^2 / (m\hbar\Omega^3)$. The bath is taken as a collection of harmonic oscillators coupled to the on-site electron density. Namely, the boson modes in Eq.(1) are labeled as $q = (\mathbf{R}, \lambda)$, where λ counts the different oscillators at site \mathbf{R} . All modes are coupled with the same strength, χ_0 , to the fermions, namely: $\hat{\chi}_q = \chi_0 |\mathbf{R}\rangle \langle \mathbf{R}|$. We take the oscillator frequencies to approach a continuum density of states (DOS) given by $\nu_B(\epsilon) \propto (\epsilon + c_2 \epsilon^2) \Theta(\epsilon)$, where c_2 parametrizes the deviation from ideal ohmic bath (realized when $c_2 = 0$).

Because of translational invariance, the steady state occupation obtained by solving Eq.(3) is a function of momentum, $f_{\alpha} \rightarrow f(\mathbf{k})$. As shown in Ref.[3], for an ohmic bath this steady state displays discontinuities of the second derivative of $f(\mathbf{k})$ at $\mathbf{k}_F^2 / (2m) = n\hbar\Omega$ for integer

n , which behave as the Fermi surface of a non-Fermi liquid state. For concreteness we will focus on the Fermi surface at $n = 1$ which is the strongest at small driving amplitudes. Notice that the effective Fermi energy is controlled by driving frequency Ω , unlike the equilibrium Fermi energy which is determined by the fermion density. Figure 2 (a-c) shows the behavior of the second order discontinuity $\delta f^{(2)} \equiv f''[\epsilon = \hbar\Omega + 0] - f''[\epsilon = \hbar\Omega - 0]$ for the $n = 1$ Fermi surface obtained directly from numerical solutions of Eq.(3) (see also Fig.1(b)), corroborating the remarkable finding of Ref.[3] that these non-analyticities remain sharp at finite bath temperature (i.e. the “ultracritical” behavior).

The strength of this emergent Fermi surface (i.e. the size of the discontinuity) is non-monotonic as a function of the bath temperature, as shown in Fig. 2 (a)-(c). At low temperatures ($k_B T_{\text{bath}} \ll \hbar\Omega$), the strength of the emergent Fermi surface first decreases rapidly with temperature and can be fit as $\delta f^{(2)}[\tau \rightarrow 0] = (a + b\tau)e^{-\tau/c}$, where $\tau = k_B T_{\text{bath}} / \hbar\Omega$ is dimensionless temperature [see Fig. 2c] (for the fit parameters see Supplementary Information (SI) section G). The size of the discontinuity in this regime saturates at large dimensionless light intensity, κ^2 , at values of order $\delta f^{(2)} \sim (\hbar\Omega)^{-2}$.

Remarkably, at higher temperatures there is a revival of the strength of the emergent Fermi surface that can peak at a temperature comparable to frequency of the drive, i.e. $k_B T_{\text{bath}} \sim \kappa\hbar\Omega$ as seen in Fig. 2(b),(f). Amazingly, this implies that the Fermi surface remains sharp at high temperatures comparable to the effective Fermi energy, and its decay at high temperatures can be approximated as a power-law: $\delta f^{(2)}[\tau \gg \tau_{\text{max}}] = a'\tau / (b' + \tau^2)$ [see Fig. 2c] (for the fit parameters see (SI) section G). Remarkably, as we will show in the next section, even such a seemingly weak non-analyticity of the occupation gives rise to quantum oscillations comparable in magnitude to those in an ordinary Fermi liquid. The presence of this higher temperature revival of the Fermi surface is ultimately controlled by the deviation from the perfectly ohmic bath, namely, for $c_2 \rightarrow 0$ the high temperature revival is absent (for the fit parameters see SI section E).

Kinetics of driven Landau levels. We will now discuss the response of the Floquet non-Fermi liquid to a magnetic field. The electron Hamiltonian from Eq.(5) is therefore modified to be:

$$\hat{h}_t = \left[\mathbf{p} - \frac{e}{\hbar} \mathbf{A}_0(\mathbf{r}) - \frac{e}{\hbar} \mathbf{A}(t) \right]^2 / (2m), \quad (6)$$

where $\nabla \times \mathbf{A}_0(\mathbf{r}) = \mathbf{B}_0$ accounts for the constant magnetic field. Solutions to Schrödinger’s associated with Eq. (6) have been discussed in quantum optics [14, 15], and can be obtained via the unitary transformation $D[\alpha(t)] = \exp[\alpha(t)\hat{a}^{\dagger} - \alpha^*(t)\hat{a}]$ where $\alpha(t) = \sum_{\xi=\pm 1} z_{\xi} e^{-i\xi\Omega t} / (\hbar\omega_c - \xi\hbar\Omega)$ with $z_{\xi} = -i\xi\Omega^{-1} \sqrt{\hbar\omega_c / (2m)} (\mathcal{E}_{\xi}^x - i\mathcal{E}_{\xi}^y)$, as follows

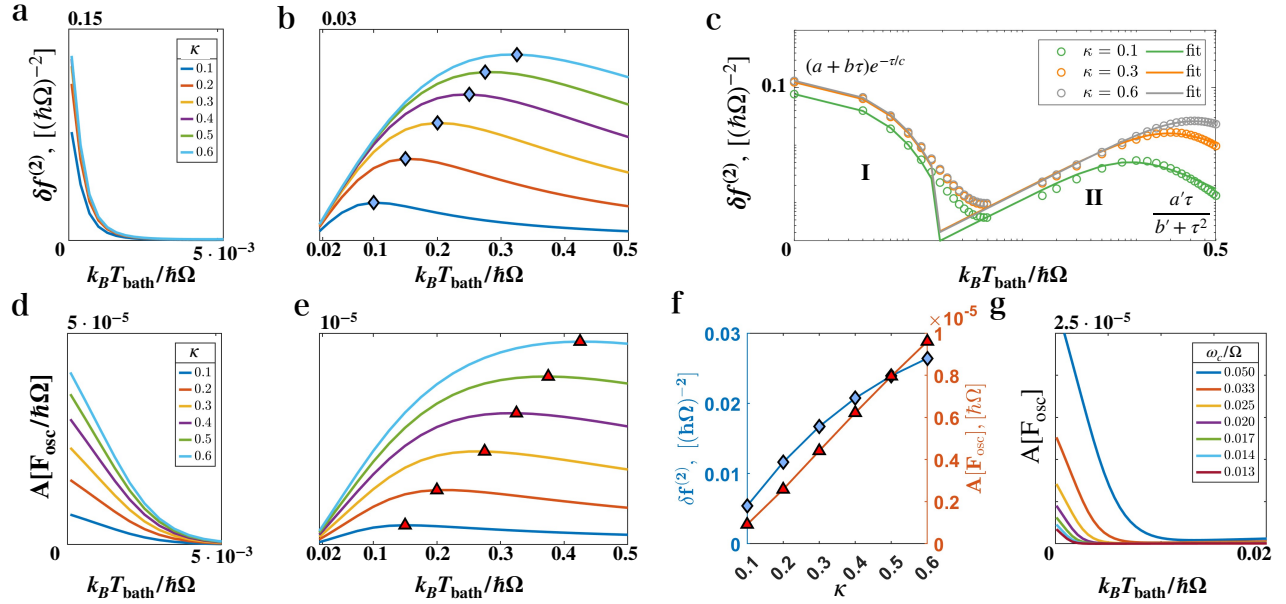


FIG. 2. Jump of the second derivative of the occupation for $\bar{n}_e = 0.8$, and various driving amplitudes κ : (a) low-temperature regime, (b) high-temperature regime (note difference in x-axis), (c) log-log plot of full temperature dependence and fits. Amplitude of the resulting quantum oscillations in the interval $\Omega/\omega_c \in [40, 43]$ in the (d) low-temperature and (e) high-temperature regimes. (f) Jump of second derivative and oscillation amplitude as a function of driving amplitude. (g) Low-temperature oscillations for different magnetic fields showing that the full width at half maximum (FWHM) scales approximately linearly with ω_c .

(see **SI** section B and Ref.[16] for more details):

$$\begin{aligned} |N, r, t\rangle &= e^{-i\Phi_N(t)} D[\alpha(t)] |N\rangle \otimes |r\rangle, \\ &= e^{-i\Phi_N(t)} \sum_{n=-\infty}^{\infty} e^{-in\Omega t} |\phi_N^n\rangle \otimes |r\rangle, \end{aligned} \quad (7)$$

where $\Phi_N(t) = E_N(t - t_0)/\hbar + (1/\hbar) \int_{t_0}^t \Delta(t') dt'$, $E_N = \hbar\omega_c(N + 1/2)$, N is the Landau level index, r is the intra-Landau level guiding center index, $\omega_c = e|\mathbf{B}_0|/m$ is the cyclotron frequency. The second line of Eq.(7), uses the Floquet theorem to express the wave-function as a sum of Floquet harmonics.

Owing to magnetic translational symmetry, the scattering rates and occupations become independent of the guiding center index r (see **SI** section A), allowing Eq. (4) to be recast as:

$$\begin{aligned} \langle W_{e,t}^{N \rightarrow N'} \rangle_T &= \frac{2\pi}{\hbar} \sum_n \int_{-\infty}^{\infty} d\epsilon \nu_B(\epsilon) |V_{NN'}^n(\epsilon)|^2 \delta(E_{N'N}^n + \epsilon), \\ |V_{NN'}^n(\epsilon)|^2 &= \frac{\chi_0^2}{4\pi^2 l_B^4} (N_b(\epsilon) + 1) Q_{NN_1}^n \quad (8) \\ Q_{NN_1}^n &= \text{Tr} \left\{ \left[\sum_m |\phi_N^m\rangle \langle \phi_{N_1}^{m-n}| \right] \left[\sum_{m'} |\phi_N^{m'}\rangle \langle \phi_{N_1}^{m'-n}| \right]^\dagger \right\}, \end{aligned}$$

where $E_{NN'}^n = E_N - E_{N'} + n\hbar\Omega$, and l_B is the magnetic length. The trace can be evaluated with the following

identity:

$$\begin{aligned} Q_{NN_1}^n &= \iint_0^1 dx dy e^{i2\pi n(x-y)} \\ &\times e^{-|\beta(x,y)|^2} L_{N_1}(|\beta(x,y)|^2) L_N(|\beta(x,y)|^2), \end{aligned} \quad (9)$$

where $L_N(x)$ is the Laguerre polynomial. For circularly polarized light: $|\beta(x,y)|^2 = 2\kappa^2(\omega_c/\Omega)[1 - \cos(2\pi(x-y))]$ (see **SI** section C for more general form). In the limit $\kappa \rightarrow 0$, Eq. (9) vanishes for $n \neq 0$, and Eq. (3) reduces to the conventional Boltzmann equation. However, the above equations are non-perturbative and valid for any value of κ . Equipped with Eq. (9) and Eq. (8), we numerically solve the Floquet-Boltzmann Eq (3).

Ultra-critical quantum oscillations. We now illustrate that the non-analyticity of the occupation indeed behaves as the Fermi surface of a non-Fermi liquid by showing that it gives rise to quantum oscillations with markedly different behavior compared to an equilibrium Fermi liquid. Quantum oscillations are expected to appear in many observables, but for concreteness we will focus on a non-equilibrium free energy defined as:

$$\frac{F}{n_e l_B^2} \equiv \frac{1}{n_e l_B^2} \sum_{N=0}^{\infty} [f_N E_N - k_B T_{\text{bath}} f_N \log f_N]. \quad (10)$$

The definition of F can be motivated by noting that in the equilibrium limit ($\kappa \rightarrow 0$) it reduces to the free energy for a system with fixed particle number that exchanges energy with a bath at temperature T_{bath} (see also [2, 17]). We

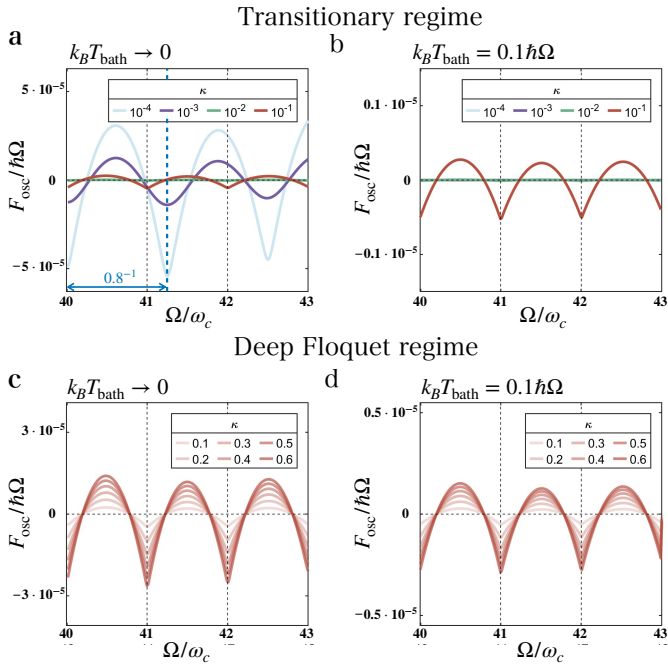


FIG. 3. (a) Quantum oscillations at small driving amplitudes, κ and low bath temperature. At $\kappa \rightarrow 0$ we see only the equilibrium quantum oscillations with a period controlled by the density, which decrease rapidly as the driving amplitude κ increases, while the new oscillations of the emergent Floquet Fermi surface with period controlled by Ω emerge. (b) At higher bath temperatures the equilibrium oscillations are exponentially suppressed and essentially invisible, and the Floquet oscillations are clearly visible and non-analytic as a function of field. At larger drive amplitudes only the Floquet quantum oscillations are visible both at (c) small and (b) large bath temperatures.

have evaluated Eq.(10) by numerically solving the Boltzmann Eq.(3) using scattering rates that are perturbative and non-perturbative in κ (see **SI** section C), and verified that both calculations give the same behavior at small κ (see **SI** section TBA). The perturbative rates are more efficient for numerical simulations, and we used them to explore in more detail the full temperature dependence.

Figure 3 shows that oscillations with a period associated with an effective Fermi energy $\hbar\Omega$ emerges as κ increases. These oscillations can be easily distinguished from the standard equilibrium oscillations which have a different period controlled by electron density, and which decrease as κ increases as a result of electron heating. One of our most remarkable findings, seen in Fig.3(b), is that these new oscillations of the emergent Floquet Fermi surface remain non-analytic as a function of *magnetic field* even when the bath is at finite temperature. This is a manifestation of their “ultra-critical” nature, namely the fact that the emergent Floquet Fermi surface remains sharp at finite temperature [3]. In equilibrium quantum

oscillations are non-analytic as a function of field only at zero temperature, and happen when the chemical potential jumps across the cyclotron gaps between Landau levels, which manifests as cusp-like features in the energy vs. filling factor plots (i.e. inverse magnetic field) [17, 18]. Therefore, what we see in Fig.3(b) is a non-equilibrium version of this behavior that amazingly remains sharp even at finite temperatures.

We have also found that the amplitude is non-monotonic as a function of temperature, as shown in Fig. 2, going first through a regime of rapid decrease with bath temperature, followed by a high temperature revival that eventually peaks at a temperature comparable with the driving frequency $\hbar\Omega$ (i.e. the effective Floquet Fermi energy), and subsequently decaying as $\sim 1/T_{\text{bath}}$ at higher temperatures. Therefore, the amplitude of oscillations is well correlated with the strength of the emergent Fermi surface, measured from the size of the jump of the second derivative at zero field, $\delta f^{(2)}$, as shown in Fig.2.

The amplitude of the Floquet quantum oscillations at low temperatures can be comparable (see **SI** section B) to the amplitude of the usual equilibrium quantum oscillations for strong light intensities $\kappa^2 \sim 1$, but it remains up to about 10% of it even down weaker intensities $\kappa^2 \sim 0.01$. On the other hand, the high temperature oscillations tend to remain relatively weaker in amplitude than the equilibrium oscillations, i.e. for $\kappa^2 = 1$ they are about 10% at their highest. The temperature width of region of high temperature oscillations is weakly dependent on magnetic field, but the temperature width of the low-temperature oscillations increases linearly with magnetic field, i.e. the latter is more similar to usual quantum oscillations [17, 18]. All of the above substantiates the idea that the non-analyticity behave as an emergent Fermi surface, which governs the observed oscillatory behavior at small magnetic fields, and that can retain quantum features even up to remarkably elevated temperatures.

Summary. We derived a Floquet-Boltzmann kinetic equation for the occupation of states in a periodically driven fermionic system coupled to an ohmic bosonic bath. We demonstrated that its solutions display non-analyticities at certain momenta which behave like emergent Fermi surfaces, by showing that they give rise to quantum oscillations of observables in the presence of magnetic fields. These oscillations have many remarkable differences with respect to equilibrium quantum oscillations, e.g. their period is controlled by the driving frequency (not the electron density), they are non-analytic as a function of magnetic field, non-monotonic as a function of temperature, can survive up to extremely high temperatures comparable to the driving frequency, and their size can be comparable to those in equilibrium.

Acknowledgements. We acknowledge support by the Deutsche Forschungsgemeinschaft (DFG) through research grant project numbers 542614019; 518372354; 555335098 (IS).

[1] O. Matsyshyn, J. C. Song, I. Sodemann, and L.-k. Shi, Fermi-dirac staircase occupation of floquet bands and current rectification inside the optical gap of metals: An exact approach, *Physical Review B* **107**, 195135 (2023).

[2] L.-k. Shi, O. Matsyshyn, J. C. Song, and I. S. Villadiego, Floquet fermi liquid, *Physical Review Letters* **132**, 146402 (2024).

[3] L.-k. Shi, O. Matsyshyn, J. C. W. Song, and I. S. Villadiego, Ultracritical floquet non-fermi liquid, *Phys. Rev. Lett.* **134**, 196401 (2025).

[4] D. Shoenberg, *Magnetic oscillations in metals* (Cambridge university press, 2009).

[5] F. T. Vasko and O. E. Raichev, *Quantum kinetic theory and applications* (Springer, 2005).

[6] A. Lazarides, A. Das, and R. Moessner, Periodic thermodynamics of isolated quantum systems, *Physical review letters* **112**, 150401 (2014).

[7] A. Lazarides, A. Das, and R. Moessner, Equilibrium states of generic quantum systems subject to periodic driving, *Physical Review E* **90**, 012110 (2014).

[8] A. Lazarides, A. Das, and R. Moessner, Fate of many-body localization under periodic driving, *Physical review letters* **115**, 030402 (2015).

[9] V. Khemani, A. Lazarides, R. Moessner, and S. L. Sondhi, Phase structure of driven quantum systems, *Physical review letters* **116**, 250401 (2016).

[10] K. I. Seetharam, C.-E. Bardyn, N. H. Lindner, M. S. Rudner, and G. Refael, Controlled population of floquet-bloch states via coupling to bose and fermi baths, *Physical Review X* **5**, 041050 (2015).

[11] M. Genske and A. Rosch, Floquet-boltzmann equation for periodically driven fermi systems, *Physical Review A* **92**, 062108 (2015).

[12] I. Esin, M. S. Rudner, G. Refael, and N. H. Lindner, Quantized transport and steady states of floquet topological insulators, *Physical Review B* **97**, 245401 (2018).

[13] K. I. Seetharam, C.-E. Bardyn, N. H. Lindner, M. S. Rudner, and G. Refael, Steady states of interacting floquet insulators, *Physical Review B* **99**, 014307 (2019).

[14] S. M. Roy and V. Singh, Generalized coherent states and the uncertainty principle, *Phys. Rev. D*; (United States) **25:12**, 10.1103/PhysRevD.25.3413 (1982).

[15] C. Gerry and P. Knight, *Introductory Quantum Optics* (Cambridge University Press, 2004).

[16] L.-k. Shi, Algebraic exact solution for driven landau levels in two-dimensional electron gases, *Phys. Rev. B* **112**, 165108 (2025).

[17] D. Shoenberg, *Magnetic Oscillations in Metals*, Cambridge Monographs on Physics (Cambridge University Press, 1984).

[18] A. A. Abrikosov, *Fundamentals of the Theory of Metals* (Courier Dover Publications, 2017).

[19] Q. Shi, P. Martin, A. Hatke, M. Zudov, J. Watson, G. Gardner, M. Manfra, L. Pfeiffer, and K. West, Shubnikov-de haas oscillations in a two-dimensional electron gas under subterahertz radiation, *Physical Review B* **92**, 081405 (2015).

SUPPLEMENTAL MATERIAL FOR “HIGH-TEMPERATURE QUANTUM OSCILLATIONS OF A NON-EQUILIBRIUM NON-FERMI LIQUID”

Appendix A: Scattering amplitudes in Landau levels

In this section, we provide a detailed procedure for performing the summation over the guiding center index. In the undriven Landau level problem, states are labeled as $|\alpha\rangle \equiv |N, r\rangle$, where N is the main Landau level cyclotron index, and r is the guiding center index. Due to magnetic translational invariance, we will show that scattering rates that appear in the kinetic equation can be effectively reduced to depend only on N , and the steady state occupation can be taken to only depends on N . We also use the equal coupling strength for all the bath modes in the system with $\hat{\chi}_q = \chi_0 |\mathbf{R}\rangle \langle \mathbf{R}|$, where $|\mathbf{R}\rangle$ is a fermion position eigenket and $\int_{\mathbf{R}} \equiv \int d^d \mathbf{R} / V$, which we introduced in the main text. Following Eq.(4) from the main text, our task is to evaluate the Floquet matrix element:

$$\int_{\mathbf{R}} \sum_{rr_1} \left| \sum_l \langle \phi_{N,r}^l | \chi_q | \phi_{N_1,r_1}^{l-p} \rangle \right|^2 = \chi_0^2 \int_{\mathbf{R}} \sum_{rr_1} \left| \sum_l \langle \phi_{N,r}^l | \mathbf{R} \rangle \langle \mathbf{R} | \phi_{N_1,r_1}^{l-p} \rangle \right|^2. \quad (\text{A-1})$$

We employ the identity $|\mathbf{R}\rangle \langle \mathbf{R}| = \delta(\mathbf{R} - \hat{\mathbf{R}}) = (1/A) \sum_q e^{iq(\mathbf{R} - \hat{\mathbf{R}})}$, where the position operator can be decomposed as $\hat{\mathbf{R}} = \hat{\mathbf{R}}_c + \hat{\mathbf{R}}_r$ into orbital, with $\hat{R}_c^x = l_B(\hat{a} + \hat{a}^\dagger)/\sqrt{2}$, $\hat{R}_c^y = -il_B(\hat{a} - \hat{a}^\dagger)/\sqrt{2}$, and guiding center index contributions with $\hat{R}_m^x = l_B(\hat{b} + \hat{b}^\dagger)/\sqrt{2}$, $\hat{R}_m^y = il_B(\hat{b} - \hat{b}^\dagger)/\sqrt{2}$ where \hat{b} (\hat{b}^\dagger) are the guiding-center ladder operators. Thus we write:

$$\sum_{rr_1} \left| \sum_l \langle \phi_{N,r}^l | \chi_q | \phi_{N_1,r_1}^{l-p} \rangle \right|^2 = \chi_0^2 \sum_{rr_1} \sum_{ll'} \langle \phi_{N,r}^l | \mathbf{R} \rangle \langle \mathbf{R} | \phi_{N_1,r_1}^{l-p} \rangle \langle \phi_{N_1,r_1}^{l-p} | \mathbf{R} \rangle \langle \mathbf{R} | \phi_{N,r}^{l'} \rangle \quad (\text{A-2})$$

$$= \chi_0^2 \sum_{ll'} \sum_r \langle \phi_{N,r}^l | \mathbf{R} \rangle \langle \mathbf{R} | \phi_{N,r}^{l'} \rangle \sum_{r_1} \langle \mathbf{R} | \phi_{N_1,r_1}^{l-p} \rangle \langle \phi_{N_1,r_1}^{l-p} | \mathbf{R} \rangle, \quad (\text{A-3})$$

which can be further simplify by employing:

$$\sum_r \langle \phi_{N,r}^l | \mathbf{R} \rangle \langle \mathbf{R} | \phi_{N,r}^{l'} \rangle = \frac{1}{A} \sum_q \langle \phi_N^l | e^{iq(\mathbf{R} - \hat{\mathbf{R}}_c[a, a^\dagger])} | \phi_N^{l'} \rangle \sum_r \langle r | e^{-iq\hat{\mathbf{R}}_r[b, b^\dagger]} | r \rangle = \frac{N_\phi}{A} \langle \phi_N^l | \phi_N^{l'} \rangle \quad (\text{A-4})$$

where we used $|\phi_{N,r}^{l'}\rangle = |\phi_N^{l'}\rangle \otimes |r\rangle$ and the fact that $\text{Tr}[e^{iq\hat{\mathbf{R}}_r}] = N_\phi \delta_{q,0}$. By substitution of Eq.(A-4) into Eq.(4) we obtained Eq.(8) of the main text.

Appendix B: Non-perturbative driven Landau Levels

Here we discuss the details of the kinetics of driven Landau levels. First, we rewrite the Hamiltonian in Eq.(6) in its operator form as:

$$\hat{h}_t = \left[\hat{\mathbf{p}} - \frac{e}{\hbar} \mathbf{A}_0 - \frac{e}{\hbar} \mathbf{A}(t) \right]^2 / (2m), = \hbar\omega_c (1/2 + \hat{a}^\dagger \hat{a}) - \hat{a}z_t^* - \hat{a}^\dagger z_t + c_t, \quad (\text{B-1})$$

where

$$z_t = \sqrt{\frac{\hbar\omega_c}{2m}} (A^x(t) - iA^y(t)) = z_+ e^{-i\Omega t} + z_- e^{i\Omega t}, \quad \mathbf{A}(t) = -\frac{i}{\Omega} \mathcal{E}_+ \exp(-i\Omega t) + \frac{i}{\Omega} \mathcal{E}_- \exp(i\Omega t), \quad (\text{B-2})$$

$$\mathbf{B} = \nabla \times \mathbf{A}_0, \quad a^\dagger |N\rangle = \sqrt{N+1} |N+1\rangle, \quad a |N\rangle = \sqrt{N} |N-1\rangle, \quad (\text{B-3})$$

$$z_+ = -\frac{i}{\Omega} \sqrt{\frac{\hbar\omega_c}{2m}} (\mathcal{E}_+^x - i\mathcal{E}_+^y), \quad z_- = \frac{i}{\Omega} \sqrt{\frac{\hbar\omega_c}{2m}} (\mathcal{E}_-^x - i\mathcal{E}_-^y), \quad c_t = \frac{e^2 \mathbf{A}(t)^2}{2m\hbar^2}. \quad (\text{B-4})$$

We proceed by performing the unitary displacement transformation $D = \exp[\alpha a^\dagger - \alpha^* a]$ with $D^\dagger = D^{-1}$ [16]. In order to explicitly show the displacement transformation, we will employ two useful identities. First is the special form of the Baker–Campbell–Hausdorff formula known as Campbell identity, which explicitly reads as

$$e^X Y e^{-X} = Y + [X, Y] + \frac{1}{2!} [X, [X, Y]] + \frac{1}{3!} [X, [X, [X, Y]]] + \dots \quad (\text{B-5})$$

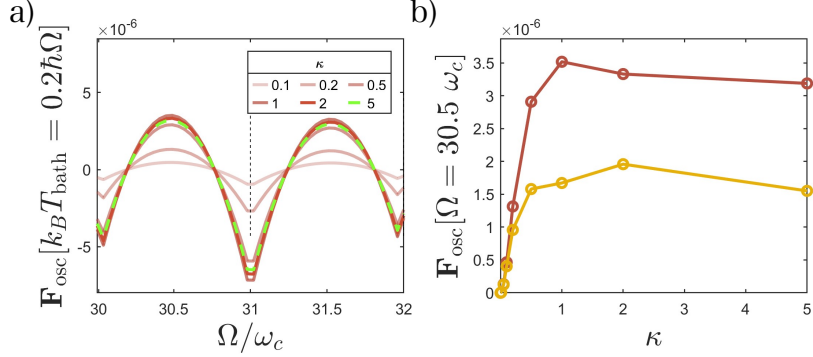


FIG. B-4. a) Non-perturbative Free energy oscillations at $k_B T_{\text{bath}} = 0.2\hbar\Omega$ for $d = 1$. b) Amplitude of the oscillations at $\Omega = 30.5\omega_c$ for $n_e = 0.8$ (red), 1.8 (yellow).

which in our case allows to write:

$$D^\dagger a D = Y + [X, Y] = a + \alpha \quad D^\dagger a^\dagger D = Y + [X, Y] = a^\dagger + \alpha^*. \quad (\text{B-6})$$

Further we use:

$$\frac{de^{-\beta X(t)}}{dt} = - \int_0^\beta e^{-(\beta-u)X(t)} \frac{dX(t)}{dt} e^{-uX(t)} du, \quad (\text{B-7})$$

noting that as $d_t X$ generally does not commute with X . By proceeding and employing the Campbell identity once again we find:

$$-i\hbar D^\dagger d_t D = i\hbar \left(\frac{dX(t)}{dt} + \frac{1}{2} \left[X(t), \frac{dX(t)}{dt} \right] \right) = i\hbar \left(\dot{\alpha}^* a - \dot{\alpha} a^\dagger + \frac{1}{2} (\alpha \dot{\alpha}^* - \alpha^* \dot{\alpha}) \right). \quad (\text{B-8})$$

By choosing:

$$\alpha(t) = \alpha_+ e^{-i\Omega t} + \alpha_- e^{i\Omega t} = \frac{1}{\hbar} \left[\frac{z_+}{\omega_c - \Omega} e^{-i\Omega t} + \frac{z_-}{\omega_c + \Omega} e^{i\Omega t} \right] \quad (\text{B-9})$$

we finally arrive to the displaced Hamiltonian

$$H'_{\text{LL}} = D^\dagger H_{\text{LL}} D - i\hbar D^\dagger d_t D \quad (\text{B-10})$$

$$= \hbar\omega_c \left(a^\dagger a + \frac{1}{2} \right) + \underbrace{\frac{\mathbf{A}_1(t)^2}{2m} - \frac{1}{\hbar} \left[\frac{|z_+|^2}{\omega_c - \Omega} + \frac{|z_-|^2}{\omega_c + \Omega} + \frac{\omega_c}{\omega_c^2 - \Omega^2} (z_+ z_-^* e^{-2i\Omega t} + z_+^* z_- e^{2i\Omega t}) \right]}_{\Delta(t)}, \quad (\text{B-11})$$

which is consistent with our previous study [2]. We can absorb the time dependent constant part of the Hamiltonian into a phase as $|\psi'(t)\rangle = e^{-i\Phi(t)} |\phi(t)\rangle$ with $\Phi(t) = \Phi_0 + \int_{t_0}^t \Delta(t') dt'$. Then the Floquet Landau levels kinetics is mapped onto the standard Landau Level problem, with the full set of solutions labeled by N, r , written in Eq.(7) of the main text. Notice, since $\Delta(t)$ is independent of Landau level index, the Floquet Boltzmann equation is unaffected by such phase factor. This can be seen from the fact that in any collision term, the evolution matrix everywhere comes in pair from $t \rightarrow t'$ and $t' \rightarrow t$, thus such Δ -related phases cancel.

Appendix C: Evaluation of the trace in Eq.(9) of the main text and perturbative limit

Here we show the details of Eq.(9) derivation in the main text. First, we write by the definition

$$\sum_{c'} |\phi_N^{c'}\rangle \langle \phi_{N_1}^{c'-d}| = \int_0^T \int_0^T \frac{dt dt'}{T^2} \left[\sum_{c'} e^{ic'\Omega(t-t')} \right] e^{id\Omega t'} |N, \alpha(t)\rangle \langle N_1, \alpha(t')| \quad (\text{C-1})$$

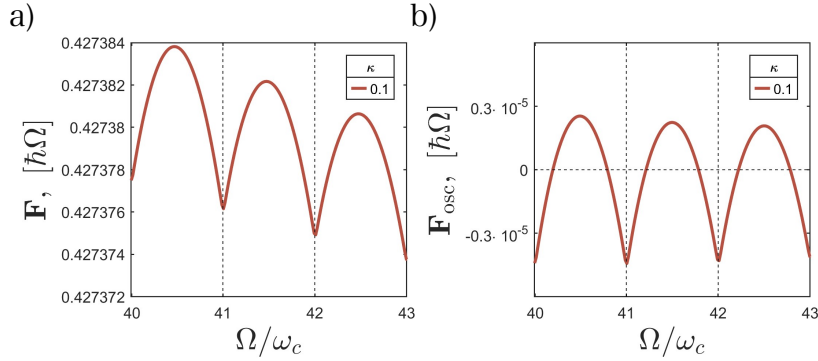


FIG. C-5. a) Full free energy variations as in Eq.(10) of the main text. b) Isolated oscillatory component.

where $|N, \alpha(t)\rangle \equiv D[\alpha(t)]|N\rangle$ and we recognize the Poisson summation formula:

$$\sum_{c'=-\infty}^{\infty} e^{ic'\Omega(t-t')} = \frac{2\pi}{\Omega} \sum_{n=-\infty}^{\infty} \delta\left(t-t' - \frac{2\pi n}{\Omega}\right) = T \sum_{n=-\infty}^{\infty} \delta\left(t-t' - nT\right) = T\delta(t-t') \quad (\text{C-2})$$

note, we used $-T < t - t' < T$ since $t \in [0, T)$, simplifying to

$$\sum_{c'} |\phi_N^{c'}\rangle \langle \phi_{N_1}^{c'-d}| = \int_0^T \frac{dt}{T} e^{id\Omega t} |N, \alpha(t)\rangle \langle N_1, \alpha(t)|. \quad (\text{C-3})$$

Next, we employ the orthogonality condition [14]:

$$\langle N, \alpha(t') | N, \alpha(t) \rangle = \exp \left\{ \frac{1}{2} \left[\alpha(t')^* \alpha(t) - \alpha(t') \alpha(t)^* \right] - \frac{1}{2} |\alpha(t) - \alpha(t')|^2 \right\} L_N(|\alpha(t) - \alpha(t')|^2). \quad (\text{C-4})$$

and straightforwardly find Eq.(9) of the main text where

$$\beta(x, y) = \frac{1}{\hbar} \left[\frac{z_+}{\omega_c - \Omega} (e^{-i2\pi x} - e^{-i2\pi y}) + \frac{z_-}{\omega_c + \Omega} (e^{i2\pi x} - e^{i2\pi y}) \right]. \quad (\text{C-5})$$

Finally, for the case of the circularly polarized light z_+ or z_- vanishes (RHS/LHS light polarization), and we write the simplified Floquet Boltzmann equation as

$$0 = \sum_{N=0}^{\infty} \left\{ (1 - f_{N_1}) f_N \sum_{p=-\infty}^{\infty} w_{N, N_1}^p S[\epsilon_N^F - \epsilon_{N_1}^F + p\Omega] - (N_1 \leftrightarrow N) \right\}, \quad (\text{C-6})$$

$$S[X] = \nu_B[X](N[X] + 1)\Theta[X] + \nu_B[-X]N[-X]\Theta[-X], \quad (\text{C-7})$$

$$w_{N, N_1}^d = \int_0^1 du \cos[2\pi du] e^{-\gamma(u)} L_{N_1}[\gamma(u)] L_N[\gamma(u)], \quad \gamma(u) = 2R_+(1 - \cos[2\pi u]) \quad (\text{C-8})$$

note $w_{N, N_1}^{-d} = w_{N, N_1}^d$ and

$$R_+ = \frac{|z_+|^2}{(\omega_c - \Omega)^2} + \frac{|z_-|^2}{(\omega_c + \Omega)^2} \approx \frac{|z_+|^2}{\hbar^2 \Omega^2} + \frac{|z_-|^2}{\hbar^2 \Omega^2} \quad (\text{C-9})$$

where $\kappa^2 = R_+ \Omega / \omega_c$ is magnetic field independent, positively defined strength of the periodic drive. To see this explicitly employ:

$$\|z_+\|^2 = \frac{\hbar \omega_c e^2}{2m\Omega^2} (\|E_\Omega\|^2 + i[\mathbf{E}_\Omega \times \mathbf{E}_{-\Omega}]), \quad \|z_-\|^2 = \frac{\hbar \omega_c e^2}{2m\Omega^2} (\|E_\Omega\|^2 - i[\mathbf{E}_\Omega \times \mathbf{E}_{-\Omega}]), \quad (\text{C-10})$$

that follow from Eqs.(B-2-B-4).

Critically, in non-perturbative fashion we find saturation of the Floquet oscillations amplitude with amplitude of the drive at $\kappa \sim 1$. The non-perturbative regime is extremely numerically heavy and is out of the scope of current study.

From Eq.(C-8) we obtain the scattering rate perturbative in the strength of the drive κ which is consistent with our previous study [2]:

$$w_{N,N_1}^d = \begin{cases} 1 - 2(1 + N_1 + N) (|\alpha_+|^2 + |\alpha_-|^2) + O(\mathcal{E}^4), & d = 0, \\ (1 + N_1 + N) (|\alpha_+|^2 + |\alpha_-|^2) + O(\mathcal{E}^4), & d = \pm 1, \\ 0 + O(\mathcal{E}^4), & |d| \geq 2. \end{cases} \quad (\text{C-11})$$

Appendix D: Oscillation extraction

In this section we discuss the numerical calculation of the Floquet free energy oscillations introduced in Eq.(10) of the main text. We begin by fixing of the total particle density for each magnetic field. In 2D electron gas at $T = 0$, the electron density is related to the Fermi energy as $\mu = \pi\hbar^2 n_e/m$, while the Landau level degeneracy per area is $N_\phi/A = eB/h = eB/(2\pi\hbar)$ with the cyclotron frequency $\omega_c = eB/m$. Thus we impose the normalization:

$$\lim_{B \rightarrow 0} \frac{N_\phi}{A} \sum_N f(N) = n_e = \frac{m\mu}{\pi\hbar^2} = \left[\frac{N_\phi}{A} \right] \frac{m\mu A}{\pi\hbar^2 N_\phi} = \left[\frac{N_\phi}{A} \right] \frac{2m\mu}{\hbar e B} = \left[\frac{N_\phi}{A} \right] \frac{2\mu}{\hbar\omega_c}. \quad (\text{D-1})$$

The quantity for which we compute the oscillations is the following effective free energy:

$$F = E - T_{\text{bath}} S = E - k_B T_{\text{bath}} N_\phi \sum_N f_N \log f_N, \quad \frac{F}{n_e A \hbar \Omega} = \frac{\omega_c^2}{\Omega^2 \mu} \sum_N \left(N + 1/2 - \frac{k_B T}{\omega_c} \log f_N \right) f(\epsilon_N). \quad (\text{D-2})$$

To extract the strictly oscillatory part, we further subtract the non-oscillatory (Landau diamagnetic) component to identify the quantum oscillations see Fig.C-5.

Appendix E: Ohmic Bath Quantum oscillations

Here we show that for a perfectly ohmic bath (i.e $c_2=0$), the “high temperature oscillations” are absent. This is consistent with the results of Ref[[3]], which found that the second derivative discontinuity for the perfectly Ohmic bath is only sharp when the bath is at zero temperature and it is smeared out when the bath is at finite temperature. In agreement with this, we find that the quantum oscillations only are present in the low temperature regime in this case, as shown in Fig.E-6.

Appendix F: Oscillations Floquet regime phase shift

We contrast the oscillation phases in the deep Floquet regime to the equilibrium quantum oscillations. To do this we choose the electron density and the driving frequency to have a value such that the area of the usual equilibrium Fermi surface and the Floquet Fermi surface are identical, and thus their quantum oscillations frequency is the same. The idea is that this allows us to contrast more easily their phase to determine if there are any changes. We find, however, that the phase as a function of magnetic field is preserved during the transition from usual oscillations which occurs as the driving amplitude, κ , increases, as shown in FIG.G-7, which illustrates that minima and maxima do not shift as the amplitude of the drive, κ increases. Therefore, the phase of these of oscillations is not consistent with the one observed in the regime of coexistence of MIRO and SdH oscillations reported in Ref.[19].

Appendix G: Fit parameters for the low and hight temperature discontinuity behavior

Here we present values of the parameter fit to for the low and hight temperature occupation function discontinuity fits, see Table G-I.

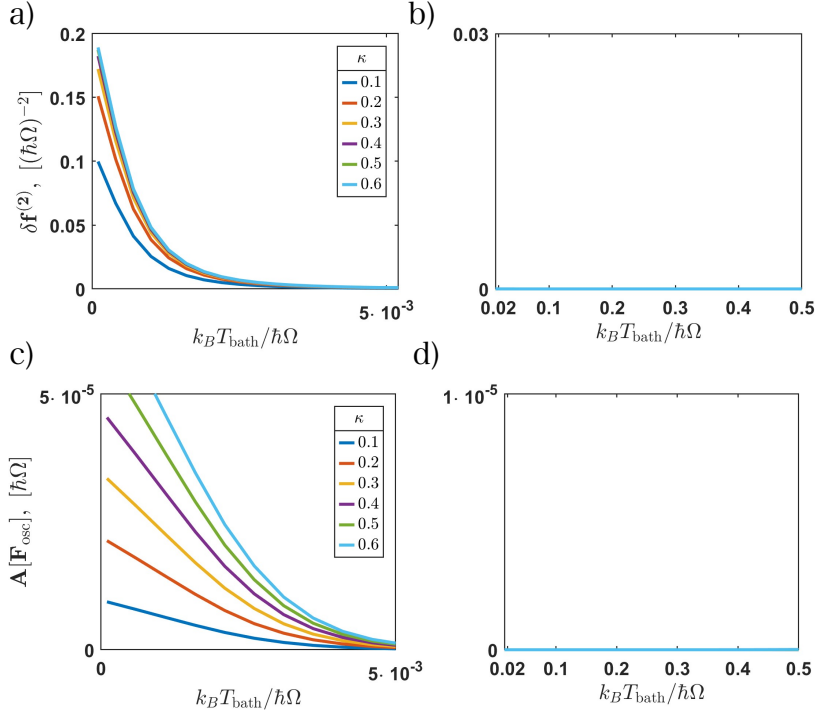


FIG. E-6. The jump of the second order derivative of the occupation function at $k = k_F$ (a-b) and the amplitude of the quantum oscillation for the perfectly ohmic bath $c_2 = 0$ as a function of the bath temperature for various strengths of the drive for $\bar{n}_e = 0.8$, $\Omega/\omega_c \in [40, 43]$ (c-d). Contrast with Fig. 2 of the main text.

κ	Low temperature fit			Higher temperature fit	
	a	b	c	a'	b'
0.1	0.097	0.3	4.4×10^{-4}	9×10^{-4}	8×10^{-3}
0.3	0.15	-0.7	4.4×10^{-4}	6×10^{-3}	3.6×10^{-2}
0.4	0.165	1.06	4.4×10^{-4}	1.6×10^{-2}	0.1

TABLE G-I. Fitted values of parameters for the jump of the second order derivative in region I (low temperature) with $\delta f^{(2)}[\tau \rightarrow 0] = (a + b\tau)e^{-\tau/c}$ and region II (hight temperature) with $\delta f^{(2)}[\tau \gg \tau_{\text{max}}] = a'\tau/(b' + \tau^2)$. For the comparison of the fit to numerically simulated data see Fig. 3c.

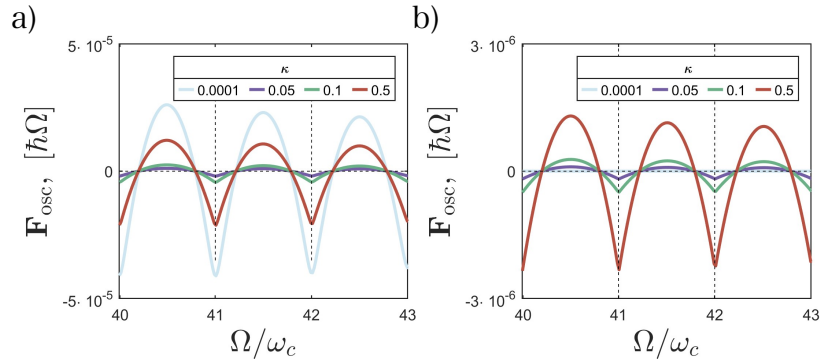


FIG. G-7. a) Low temperature $k_B T_{\text{bath}} = 10^{-4} \hbar\Omega$ quantum oscillations. We find that the phase is unchanged by a transition from the usual equilibrium oscillations (blue line) to the Floquet regime (red line). b) High temperature regime $k_B T_{\text{bath}} = 0.1 \hbar\Omega$. We find exponentially suppressed (close to $F_{\text{osc}} = 0$ line) equilibrium oscillations, while the Floquet controlled component grows with the strength of the drive. Here we set $\bar{n}_e = 1$ ensuring that the usual equilibrium Fermi energy is $\hbar\Omega$.